ISSN 0869-5911, Petrology, 2008, Vol. 16, No. 3, pp. 211–231. © Pleiades Publishing, Ltd., 2008.
Original Russian Text © E.V. Bibikova, S.B. Lobach-Zhuchenko, G.V. Artemenko, S. Claesson, A.V. Kovalenko, I.N. Krylov, 2008, published in Petrologiya, 2008, Vol. 16, No. 3, pp. 227–247.

Late Archean Magmatic Complexes of the Azov Terrane, Ukrainian Shield: Geological Setting, Isotopic Age, and Sources of Material

E. V. Bibikova[a], S. B. Lobach-Zhuchenko[b], G. V. Artemenko[c], S. Claesson[d], A. V. Kovalenko[b], and I. N. Krylov[b†]

[a] *Vernadsky Institute of Geochemistry and Analytical Chemistry, Russian Academy of Sciences, ul. Kosygina 19, Moscow, 117975 Russia*
e-mail: bibikova@geokhi.ru

[b] *Institute of Precambrian Geology and Geochronology, Russian Academy of Sciences, nab. Makarova 2, St. Petersburg, 199034 Russia*

[c] *Institute of Geochemistry, Mineralogy, and Ore Genesis, National Academy of Sciences of Ukraine, prosp. Palladina 34, Kiev, 03680 Ukraine*

[d] *Swedish Museum of Natural History, P.O. Box 50007, S 10405 Stockholm, Sweden*

Received February 27, 2006; in final form, August 6, 2007

Abstract—Geochemical, isotopic–geochemical, and geochronological information was obtained on magmatic rocks from the Saltychan anticlinorium in the Azov domain of the Ukrainian Shield. The rocks affiliate with the calc–alkaline series and a high-Mg series. The rocks of these series notably differ in concentrations of trace elements and REE and range from gabbro to granodiorite–quartz diorite in composition. The NORDSIM ion-probe U–Pb zircons ages of rocks belonging to the Obitochnen Complex and having both elevated and normal mg# correspond to 2908–2940 Ma. The Osipenkovskaya intrusion has an age of 2855 ± 19 Ma. The most alkaline North Obitochnen intrusion was emplaced in the Proterozoic, at 2074 ± 11 Ma. The age of the amphibolite metamorphism of the host gneisses is reliably dated at 3120–3000 Ma. The model Sm–Nd ages of the intrusive rocks do not exceed 3150 Ma. According to geochemical evidence, the parental melts of the magmatic rocks were derived from mantle domains variably enriched in lithophile elements. The results obtained by studying the Sm–Nd isotopic system corroborate the conclusion drawn from geochemical evidence that most of the melts were derived from the mildly enriched mantle, practically without involvement of ancient crustal material. The mantle became enriched in LREE at approximately 3000 Ma, which corresponds to the age of metamorphism of the supracrustal rocks. This process was separated from the derivation of the melts by a time span of 70–80 Ma. The relative age of the intrusive rocks and their variable composition can be most adequately explained by a contribution of heat and material from a plume to the derivation of the parental melts of these rocks.

DOI: 10.1134/S0869591108030016

INTRODUCTION

The Ukrainian Shield consists of Archean and Proterozoic domains. Some researchers believe that these domains (blocks) are fragments of a single craton (Shcherbak et al., 1995; Esipchuk, 2004), while others consider the shield to be a Proterozoic collage of discrete terranes (Claesson et al., 2006 and references therein).

Relatively comprehensive isotopic geochronological information is now available on the Middle Dnepr domain (Shcherbak et al., 2005; Samsonov et al., 1996). It is most difficult to reproduce the geological history of the domains composed of complicatedly tectonized high-grade metamorphic complexes, such as Podolian and Azov, in which the oldest rocks of the shield were found (Bibikova, 1989; Bibikova et al., 1982, 1990; Claesson et al., 2006). Reliable isotopic dates were obtained for the metamorphism and protolith of the oldest rocks in the Podolian domain (Bibikova et al., 1982; Claesson et al., 2006), while isotopic dates on the Azov domain are much more scarce: there are only isotopic–geochronological data on the oldest rocks of the Orekhovo–Pavlograd zone (Bibikova et al., 1990).

The Azov megablock in the southeastern part of the Ukrainian Shield (Fig. 1) is separated by the Orekhovo–Pavlograd tectonic zone from the Middle Dnepr granite–greenstone belt in the west, is bounded by the Dnepr–Donets aulacogen in the northeast [some researchers believe that the shield continues on the other side of this aulacogen and is traced to the Voronezh Massif (Artemenko et al., 1995; Glevassky and Glevasska, 2002)], and is covered by the Sea of Azov in the south. The megablock is dominated by supracrustal rocks metamorphosed to the granulite and amphibolite facies, in contrast to the Middle Dnepr granite–green-

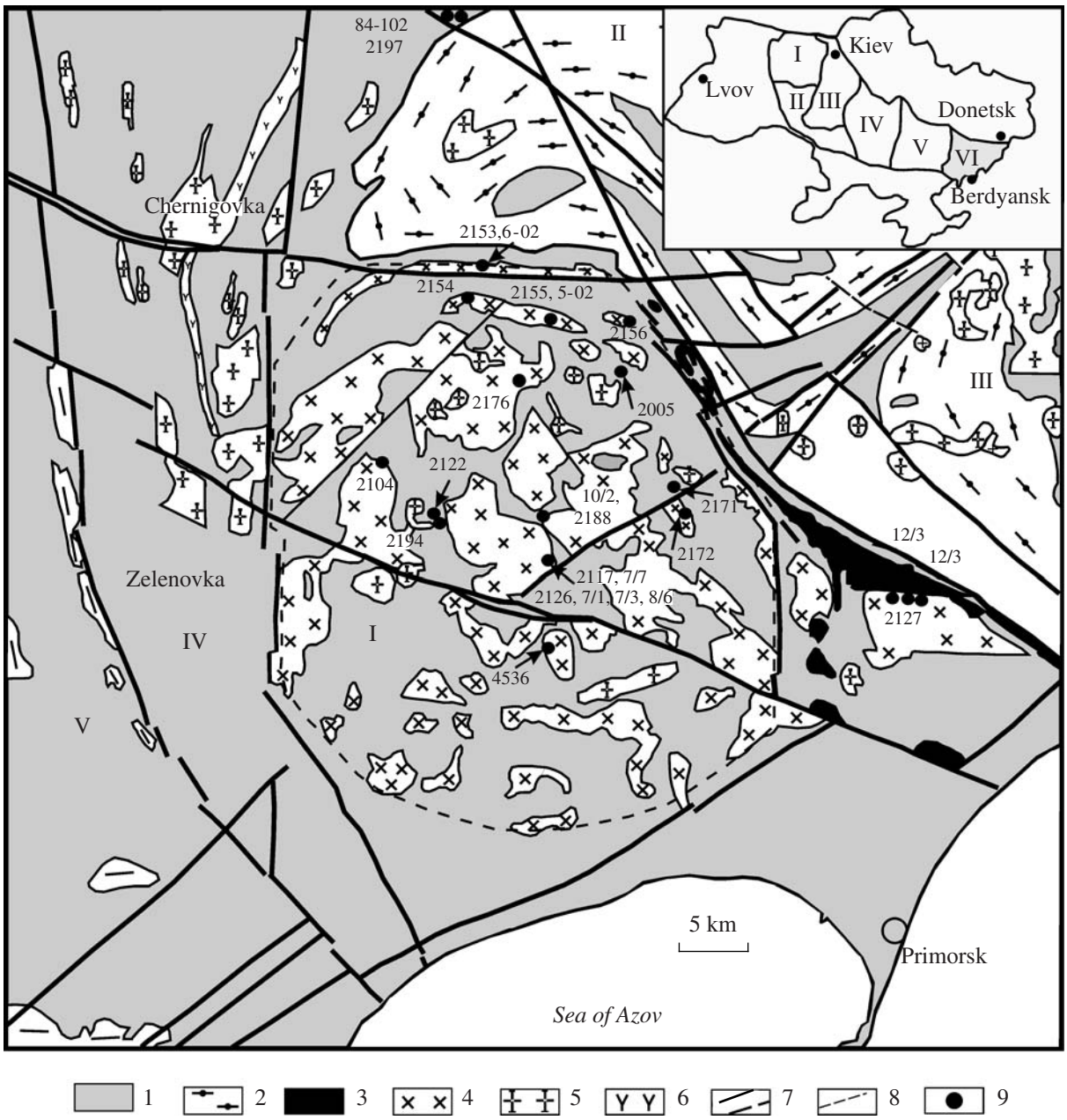

Fig. 1. Geological setting of intrusions of the Obitochnen Complex in the Saltychan anticlinorium (prepared with the use of data from Borodynya et al., 2004).

(*1*) West Azov Group; (*2*) Central Azov Group; (*3*) Osipenkovskaya Group; (*4*) Obitochnen Complex; (*5, 6*) Proterozoic intrusions: (*5*) granitoids, (*6*) carbonatites; (*7*) faults; (*8*) contour of the Obitochnen dome; (*9*) sampling sites. Geological structures: (I) Saltychan dome; (II) western slope of the Mangush synclinorium; (III) Mangush synclinorium; (IV) Lozovatskaya anticline; (V) Korsakskii syncline.

The inset shows the megablocks of the Ukrainian Shield: (I) Northwestern; (II) Dnestr–Bug; (III) Rossinsko–Tikichskii; (IV) Ingulo–Inguletskii; (V) Middle Dnepr; (VI) Azov.

stone belt south of it, whose predominant rocks are orthogneisses and intrusive tonalites and trondhjemites and where metamorphic grade of the supracrustal rocks does not exceed the amphibolite facies.

The intrusive rocks occurring in the Azov megablock are ascribed to the Archean and Proterozoic in the regional schemes, whereas the metamorphic rocks are thought to be Early Archean. The presumed age relations—the time spans between the Early Archean metamorphism and the folding of the supracrustal rocks and the latter process from the emplacement of the intrusions—put forth the problem of the geodynamic nature of the magmatism. In this context, one of the tasks of our research was formulated

as reproducing the succession of the endogenic processes and their precise isotopic dating.

Magmatism in the Azov domain was studied by many researchers (*Petrology…*, 1990; Einor et al., 1971; Tsukanov, 1977; and references therein). Analysis of the literature demonstrates that the Azov megablock includes highly magnesian rocks, which are interesting in comparison with sanukitoids, mantle derivatives whose geological setting was scrupulously examined in the Baltic and Canadian shields. Important geological–petrological problems related to the genesis of sanukitoids are their age relations with tonalites and trondhjemites and with rocks of normal mg#, i.e., those occurring together in some Archean cratons, including the Azov domain.

Our research was centered mostly on the precise U–Pb isotopic dating of intrusive rocks most of which belong to the Obitochnen Complex, as well as the classification of these rocks, with regard for the literature data, into petrochemical series for the purposes of a geodynamic model of the magmatic processes.

GEOLOGY OF THE AZOV DOMAIN AND THE SALTYCHAN MAGMATIC PROVINCE (OBITOCHNEN GABBRO–GRANODIORITE COMPLEX)

Much of the Azov domain consists of metamorphic rocks and migmatites of the West Azov and Central Azov groups. According to data obtained by several researchers, the age of the metamorphic rocks varies from the Paleoarchean (Kirilyuk et al., 2002; Polunovskii and Esipchuk, 1985) to Proterozoic (Einor et al., 1971). The marginal parts of the Western Azov domain contain tectonic fragments of greenstone belts (Fig. 1) dated at 3.2–3.0 Ga. The southern part of the Western Azov domain abounds in plutonic rocks (gabbro and diorites), which compose a large magmatic province in the central part of the Saltychan anticlinorium, over an area of approximately 1500 km^2 (*Geological Map…*, 1998). The whole territory of the Azov domain was affected by Late Archean (~2800 Ma) metamorphism and plagiomigmatization, and the eastern part of the domain contains widespread Proterozoic alkaline magmatic rocks. Available geochronological information on rocks of the Azov domain was reported in (Shcherbak et al., 1995; Artemenko et al., 2002, 2003).

The Saltychan anticlinorium is a dome-shaped structure approximately 2000 km^2 in area. Geophysical data indicate that its central part is underlain by an arch structure in the Moho discontinuity, which is interpreted as a large diapir that was traced to a depth of 60 km (Nasad et al., 2001). Small (no larger than 85 km^2) gabbro and diorite intrusions (Obitochnen Complex) (Usenko, 1960; *Petrology…,* 1990) account for more than a half of the Saltychan anticlinorium by area. The area includes widespread lamprophyre and hornblendite dikes (Ivanushko, 1973) and, along with intrusions of the Obitochnen Complex, also small intrusions and migmatites of tonalite and trondhjemite composition, which are classed with the Shevchenkovskii Complex (which was dated at 2800 Ma; Shcherbak et al., 1981). The plutonic rocks are locally deformed and sheared and, in some zones, also migmatized. These processes were responsible for the fragmentation of some of the massifs and the transformation of some of their rocks into gneisses and amphibolites, which are sometimes hardly discernible from the gneisses and amphibolites of the West Azov Group.

The Obitochnen Complex includes rocks varying from gabbro to granodiorite, with the predominance of gabbro and with diorite and quartz diorite contained in subordinate amounts. According to their composition, the rocks of the Obitochnen Complex are classified into two petrochemical series: with normal and elevated mg#. All of them are characterized by similar geological setting: they cut the metamorphic rocks and migmatites of the West Azov Group and are, in turn, intersected by tonalite–trondhjemite veins and lamprophyre dikes.

Massifs of magnesian rocks [mg# = MgO/(MgO + FeO) = 0.48–0.69] group mostly in the north and northeast of the territory, while rocks of normal mg# (0.38–0.45) are prone to be restricted to the central and western parts of the Saltychan anticlinorium. The southeastern part of this territory outside the Saltychan anticlinorium hosts the high-Mg Osipenkovskii granodiorite massif.

The largest gabbro massifs (3 × 5 km) occur in the central part of the Saltychan anticlinorium (Tsukanov, 1977). The gabbro are high- and moderate-Al, meso- and leucocratic rocks of the Na series and have mg# = 0.44–0.53 in most massifs. Some of the massifs contain more magnesian rocks with mg# = 0.62–0.67 (Table 1, Fig. 2). The gabbro with normal mg# is characterized by concentrations of Sr (520–1298 ppm) and Ba (90–240 ppm), typical of the calc–alkaline series, at low concentrations of Rb (6–10 ppm) and, correspondingly, low Rb/Sr ratios (0.01–0.02) and low concentrations of Cr and Ni, with Cr/Ni < 1 (Table 2).

The REE concentrations in the gabbro of normal and elevated mg# are similar (Table 2, Fig. 3a) at low degrees of LREE and HREE fractionation [$(La/Yb)_N$ = 7 and 5, respectively]. The geochemical differences between the calc–alkaline and magnesian gabbro affect their Cr, Cu, Th, Ti, Li, Zn, and Ga concentrations and the Ti/Zr ratio. The Th/U ratio is close to that in the mantle in the gabbro of elevated mg# and is lower in the gabbro of normal mg#. The Zr/Hf ratio in the gabbro is lower than in the mantle, and the concentrations of both Zr and Hf in the gabbro are much lower than in MORB, which are derivatives of the primitive mantle (Table 2). A distinctive compositional feature of mafic rocks form the Obitochnen Complex are clearly seen in some discriminant diagrams. In the Th/Yb–Ta/Yb diagram

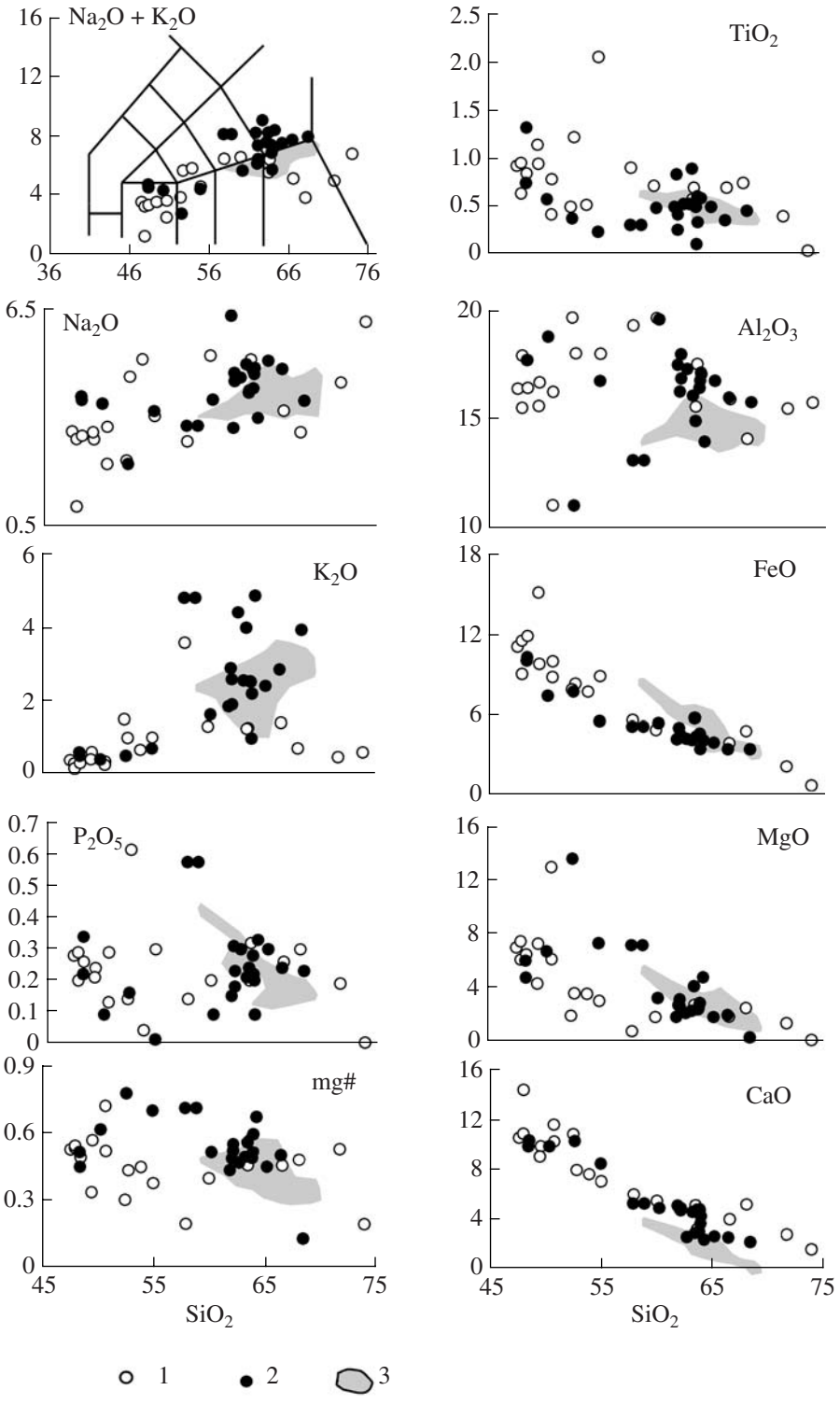

Fig. 2. SiO_2 vs. element (wt %) diagrams for intrusive rocks from the Saltychan anticlinorium, Azov megablock.
(*1*) Rocks of normal mg#; (*2*) rocks of elevated mg#; (*3*) sanukitoids from the Pilbara block, Australia (Smithies and Champion, 2000).

(Fig. 4a), both samples lie in the field of continental alkaline basalts, and samples 2107 and 2128 plot in the La–Y–Nb diagram (Fig. 4b) in the area where the fields of calc–alkaline and island-arc tholeiites overlap and at the boundary between the fields of continental and calc–alkaline basalts, respectively.

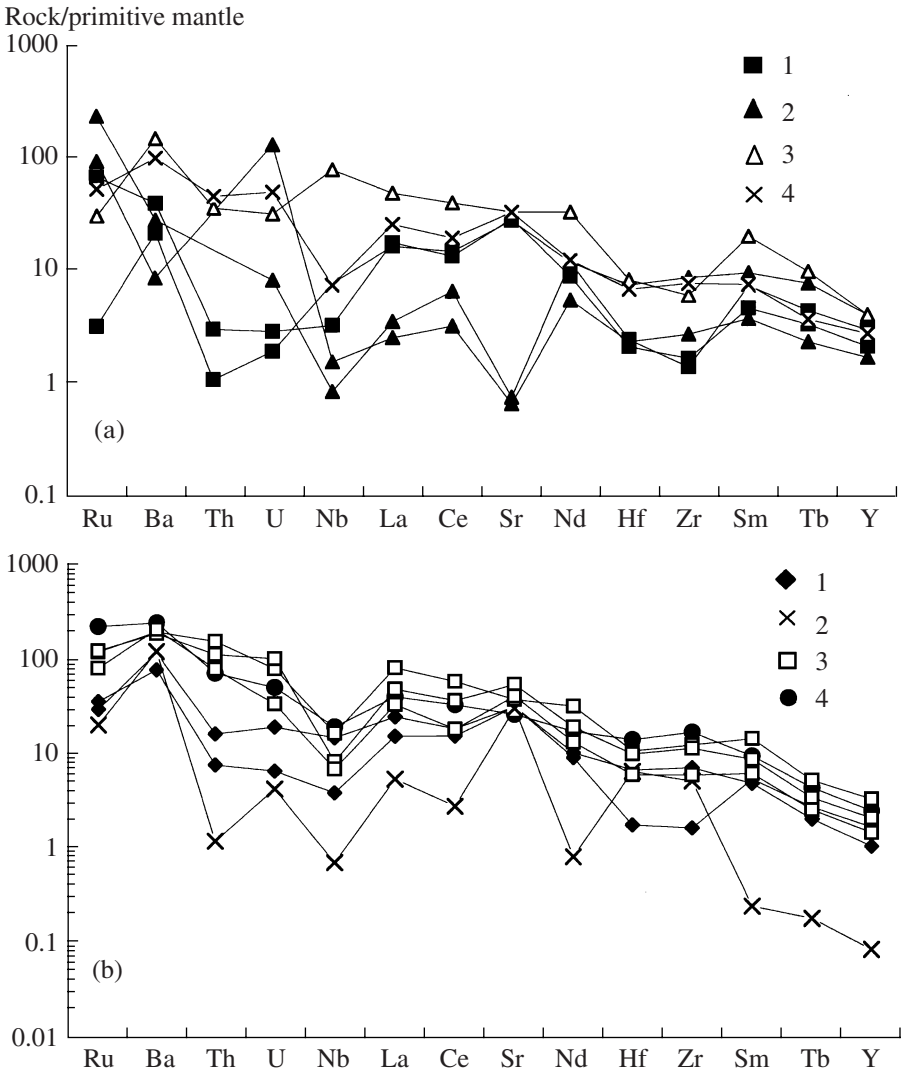

Fig. 3. Primitive mantle-normalized (Sun and McDonough, 1989) REE and trace-element patterns for magmatic rocks from the Saltychan anticlinorium, Azov megablocks.
(a) Granitoids: (*1*) Obitochnen Massif; (*2*) Shevchenkovskii Complex; (*3*) Osipenkovskii Massif; (*4*) North Obitochnen Massif.
(b) Mafic rocks: (*1*) gabbro; (*2*) high-Mg hornblendites; (*3*) Fe-rich hornblendite; (*4*) lamprophyre.

According to their chemical composition, the hornblendites are classified into two groups: high-Fe and high-Mg (Tables 1, 2). The low CaO concentration in the magnesian group suggests a significant role of orthopyroxene in the original composition of the rocks, a feature also reflected in the predominance of hypersthene in their normative composition. The Fe-rich hornblendites are characterized by elevated concentrations of Ti (up to 7 wt %), V, P, Sr, Ba, Ga, Ge, Nb, and REE compared to those in the magnesian hornblendites at similar (or even lower) Rb concentrations in the former rocks (Fig. 4a). This results in significant differences in the Rb/Sr ratios of these rocks (Tables 1, 2). The Fe-rich hornblendites are also noted for unusually high Ti/Zr ratios (250–660). Figure 4a shows that the Fe-rich group has no negative Nb anomalies. These rocks are characterized by strong fractionation of REE [$(La/Yb)_N = 18$], whereas the magnesian hornblendites are characterized by an unfractionated distribution of REE, very high Cr and Ni concentrations, and high Cr/Ni ratios. Thus, the Fe-rich hornblendites have an unusual composition: very high fe# at enrichment in incompatible elements and Ti.

As follows from the aforesaid, the mafic magmatism of the Saltychan anticlinorium gave rise to a number of rock groups with different geochemical characteristics. The comparison of some ratios of strongly incompatible elements that weakly depend on the degree of melting and later fractionation (Th/U, Ba/Th, Sr/Nd, Pb/Nd, and Nb/La; Hofmann, 2003) shows that the gabbro, Fe- and Mg-rich hornblendites were derived from different sources (Table 2).

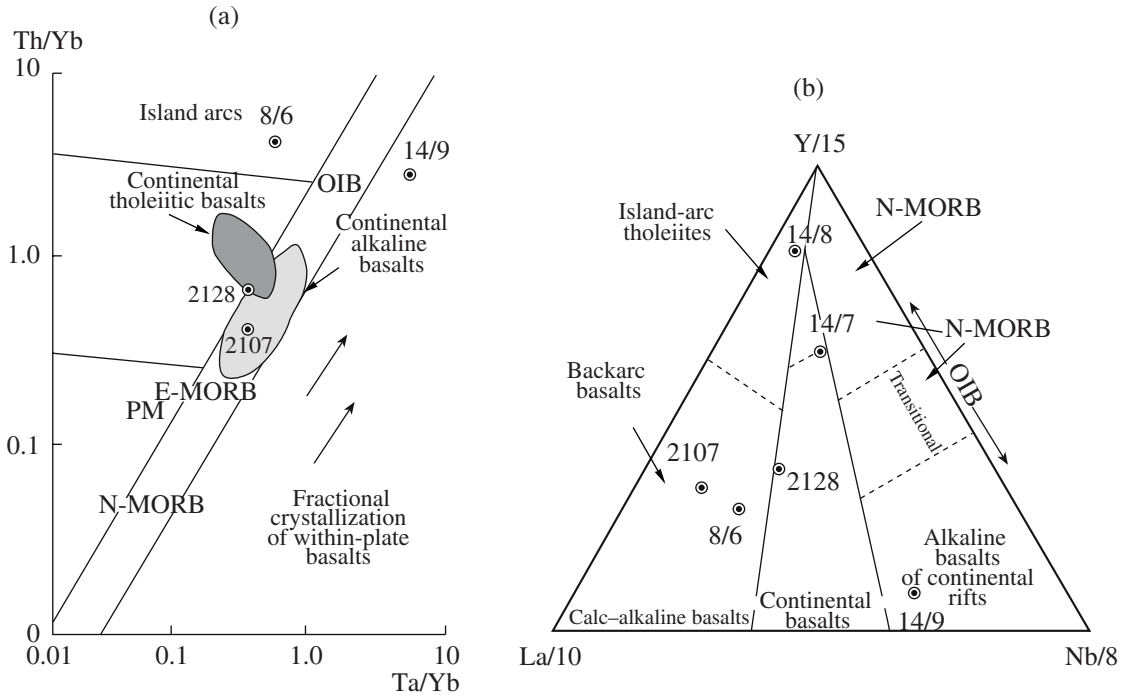

Fig. 4. Mafic rocks from the Saltychan anticlinorium in (a) Th/Yb vs. Ta/Yb and (b) La–Y–Nb (Gomes-Pugnaire et al., 2000) discriminant diagrams.

The *lamprophyres* compositionally correspond to basic and intermediate rocks (Table 1). The basic lamprophyres are low-Al rocks of elevated mg# (0.61–0.68), with Na_2O/K_2O = 6–10. The rocks have Ba (from <100 to 175 ppm), Sr (275–368 ppm), and Rb (<5 to 9 ppm) concentrations lower than in the host calc–alkaline gabbro at comparable concentrations of Zr and equally low Rb/Sr and Ti/Zr ratios. These rocks differ from all other mafites in having high Cr and very low Ni concentrations and, hence, Cr/Ni > 23, whereas this ratio of the gabbro and hornblendites is <1.

The *granitoids* of the Obitochnen Complex (except the Northern Obitochnen Massif) are mostly diorites and quartz diorites, with much lower amounts of granodiorites and quartz monzonites. The chemical composition of the rocks is reported in Table 1. Similarly to the gabbro and hornblendites, the granitoids comprise rocks of normal and elevated mg#. The latter (sanukitoids) are notably richer in K. Both rock types are characterized by low alkalinity and belong to the K–Na series. A pervasive feature of the granitoids is their affiliation with high- and very high-Al rocks.

The major-element composition of granitoids from the Obitochnen Complex is illustrated in the diagrams of Fig. 3, which also show the composition of roughly coeval sanukitoids form the Pilbara block. As can be seen in the diagrams, their compositions practically fully overlap, except higher Al_2O_3 concentrations in the Obitochnen granitoids. The latter are also characterized by a broad range of their SiO_2 concentrations, higher concentrations of alkalis, and lower concentrations of FeO. The Cr and Ni concentrations of the Obitochnen diorites and quartz diorites vary as follows: Ni = 11–130 ppm, Cr = 20–200 ppm, which reflects variations in mg#. The concentrations of lithophile elements are as follows: Rb = 15–150 ppm, Sr = 440–1350 ppm, Zr = 130–175 ppm, Ba = 450–1934 ppm (Tables 1, 2; *Petrology…*, 1990). Granitoids of the Obitochnen Complex have relatively low REE concentrations (Table 2), similar to those of the gabbro, and are characterized by positive Eu anomalies or their absence. The spidergrams (Fig. 4b) show low negative Nb, Hf, and Zr anomalies.

The Osipenkovskii Massif consists of granitoids, quartz monzonites, and syenites of variable (mostly high) mg# (Table 1). In the *Ab–Or–Qtz* diagram, the rocks of the massif plot along the calc–alkaline trend and belong to the K–Na series. Compared to the granitoids in the central part of the Saltychan anticlinorium, the rocks of the Osipenkovskii Massif have two- to threefold higher REE concentrations (Table 2) and higher contents of Rb, Sr, Zr, Ba, and Y (Tables 1, 2; Fig. 4b) and show either positive or negative Eu anomalies. Correspondingly, granites of the Osipenskovskii Massif have lower concentrations of V, Cr, Co, and Ni. With the transition from more basic to more silicic compositions, the REE concentrations decrease approximately twofold, along with a significant decrease in the concentrations of many other elements, such as Be, Sc, Pb, Th, U, Fe-group elements, and HFSE (Table 2, Fig. 4b). The high mg# of rocks of the Osipenkovskii Massif and their richness in lithophile

Table 1. Average compositions of intrusions and dikes of the Saltychan magmatic province, Azov domain

Samples and their numbers	Rock	SiO_2	TiO_2	Al_2O_3	FeO	MnO	MgO	CaO	Na_2O	K_2O	P_2O_5	LOI	mg#	Ba	V	Rb	Sr	Y	Zr
Obitochnen magmatic complex																			
Elenovskii Massif																			
n = 7	gabbro	49.7	0.87	16.19	9.87	0.12	7.25	10.7	2.64	0.4	0.26	1.17	0.57	218	183	13	504	16	87
East Eliseevskii Massif																			
n = 3	gabbro	50.1	0.72	18.94	7.51	0.08	5.76	10.3	4.17	0.5	0.15	1.17	0.66						
n = 2	diorite	54.8	2.06	18	8.89	0.09	3	7.1	3.55	1	0.3	0.99	0.38						
West Eliseevskii Massif																			
2185	gabbro	48.7	1	18.94	10.07	0.15	4.9	10.2	3.2	0.5	0.4	1.29	0.47						
n = 3	quartz diorite	58.1	1.49	16.32	7.47	0.07	3.25	5.9	4.24	0.8	0.4	0.89	0.44						
Krymskii Massif																			
n = 4	quartz diorite	58.8	0.81	19.49	5.23	0.04	1.28	5.74	4.04	2.5	0.17	1.4	0.3						
Central Obitochnen Massif																			
2154	gabbro	49.1	0.28	16.16	8.47	0.08	9.22	10.7	2.95	0.8	0.09	1.92	0.66						
5-02	quartz diorite	63.8	0.6	17.14	4.61	0.06	2.73	3.64	4.73	1	0.2	0.5	0.51	544	97	36	709	13	107
Uspenovskii Massif																			
2172	diorite	53.1	0.18	17.49	7.42	0.18	6	9.2	3.8	0.9	0.36	1	0.59						
Novotroitskii Massif																			
2158	gabbro	50.9	0.28	15.9	6.63	0.07	1.79	3.3	4.5	0.6	0.44	0.4	0.48						
Osipenkovskii Massif																			
n = 2	quartz syenite	67.1	0.25	14.03	3.44	0.07	2.23	3.62	4.89	2.8	0.2	0.98	0.48	1808	33	77	1011	7	130
n = 4	quartz monzodiorite	62.9	0.49	16.47	4.43	0.05	2.38	3.82	4.43	3.2	0.18	1.09	0.49	1713	66	105	911	14	175
North Obitochnen Massif																			
6-02	quartz syenite	64.1	0.58	13.94	4.1	0.06	4.76	2.33	3.5	4.9	0.33	0.7	0.67	2101	86	219	631	13	173
2153	quartz diorite	60.3	0.62	14.2	5.74	0.08	4.99	5.73	2.58	3.6	0.15	1.29	0.61						
Kamyshevatskii Massif																			
2156	quartz monzonite	64.2	0.62	13.67	5.18	0.15	3.79	3.54	3.2	4.1	0.42	0.7	0.57						
Intrusions, veins, and vein material of migmatites of the Shevchenkovskii Complex																			
n = 6	trondhjemite	70.7	0.17	15.81	2.36	0.03	0.82	2.5	5.19	1.1	0.24	0.67	0.37	980	24	15	718	5	92
n = 3	tonalite	66.1	0.67	15.2	5.49	0.05	2.19	4.12	3.82	0.8	0.27	0.92	0.42	805	42	21	701	12	138
Mafic dikes in gabbro of the Elenovskii Massif																			
n = 5	lamprophyre	48.7	1.05	10.7	10.7	0.19	11.6	11.7	2.16	0.4	0.26	1.52	0.66	203	213	19	329	15	98
n = 2	lamprophyre	57.4	0.51	14.33	7.51	0.12	6.21	7.17	3.41	1.3	0.24	0.94	0.6	666	172	37	770	19	105
Mafic dikes and pegmatites in rocks of the West Azov Group																			
n = 2	hornblendite	42.1	5.84	7.14	17.2	0.24	9.94	11.9	1.53	0.8	0.48	1.25	0.5	813	656	31	371	23	183
n = 3	hornblendite	51.4	0.21	4.16	13.13	0.36	20.3	6.15	0.33	0.8	0.07	1.89	0.74	204	53	100	15	15	72
n = 2	gabbro	49.2	1	13.43	11.14	0.15	8.24	10.5	3.11	0.4	0.57	0.95	0.55	413	254	13	661	17	91
16/4	lamprophyre	56.5	0.74	16.17	7.95	0.1	4.48	7.67	4.31	0.3	0.33	0.4	0.5	333	127	6	747	24	121
14/5	pegmatite I	72.4	0.07	14.8	1.59	0.24	0.31	0.7	4.8	5	tr	0.7	0.26						
14/4	pegmatite II	73.8	0.07	15.04	1.54	0.05	0.3	1.65	6.5	0.5	tr	0.4	0.26						

Note: Oxides are given in wt %, elements are in ppm, *tr* mean trace concentrations.

Table 2. Concentrations (ppm) of REE and trace elements in magmatic rocks from the Saltychan anticlinorium, Azov megablock

Element	2107	2128	4536	5-02	10/2	12/2	12/3	2127	14/8	14/7	14/9	6-02	8/6
V	216	389	104	116	24	101	62	88	84	58	715	114	126
Cr	83	65	64	28	29	23	12	9	1276	1128	45	256	172
Co	43	53	9	18	2	14	12	9	70	84	80	18	27
Ni	89	73	13	23	3	10	19	5	956	1028	74	65	7
Cu	35	62	9	7	3	20	n.a.	1	n.a.	n.a.	121	15	1.4
Zn	83	131	48	57	1	68	n.a.	65	n.a.	n.a.	244	59	85
Ga	18	22	16	18	16	18	42	18	12	7	19	17	18
Ge	n.a.	n.a.	n.a.	n.a.	n.a.	n.a.	5.9	n.a.	9	7	19	n.a.	n.a.
Rb	42	2	19	23	13	77	79	52	147	58	19	143	33
Sr	608	587	686	685	658	821	1180	888	16	14	699	568	694
Y	10	14	5	8	0.4	16	10	7	19	8	19	12	13
Zr	19	16	83	19	60	145	134	70	98	31	68	198	87
Nb	2.3	5.4	10.7	2.8	0.5	12	6	5	0.6	1.1	55	14	5.2
Cs	1.48	0.81	3.2	1	0.65	1.3	0.94	1.11	25.7	9.3	8.4	8	2.95
Li	50	27	11	27	2.1	9.3	n.a.	12.3	n.a.	n.a.	42.4	43	22.1
Be	0.6	0.7	0.8	0.7	0.73	1.9	n.a.	1.5	n.a.	n.a.	2	2.6	1.2
Sc	24.9	23.9	6.9	9.3	0.2	6	n.a.	4	n.a.	n.a.	32.5	10.2	27.5
Ba	272	147	832	549	858	1382	1337	1475	193	59	1026	1731	687
Pb	14	2	6	4.5	5	20	n.a.	14	n.a.	n.a.	3	27	7
La	12.4	11.5	17.8	11.1	3.9	58.9	35	24	2.49	1.79	34	29	18
Ce	24.4	26.9	34.7	28.9	5.21	110	69	34.3	11.9	5.9	72.3	62	35.3
Pr	3	3.8	3.8	3.1	0.42	13	7.3	5.24	2.8	1.4	10.2	6.6	4.45
Nd	12.1	16.1	14.5	12.9	1.13	45.2	27.2	18.8	16.1	7.5	45.1	24.5	16.9
Sm	2.1	3.3	2.27	2.53	0.11	6.75	4.1	2.89	4.3	1.7	9.07	4.44	3.4
Eu	0.73	1.11	1.29	0.81	0.36	1.58	1.56	1	1.49	0.55	2.6	1.19	0.93
Gd	2.2	2.92	1.77	2.26	0.07	4.73	3.5	2.05	4.4	1.8	7.9	3.19	2.76
Tb	0.37	0.49	0.23	0.31	0.02	0.6	0.39	0.29	0.85	0.26	1.08	0.5	0.41
Dy	1.88	2.64	1.14	1.55	0.06	2.81	1.8	1.37	4	1.3	4.53	2.08	2.07
Ho	0.42	0.62	0.21	0.3	0.02	0.55	0.32	0.25	0.77	0.23	0.86	0.43	0.44
Er	1.07	1.61	0.51	0.8	0.06	1.56	1.08	0.73	2.1	0.74	1.97	1.24	1.32
Tm	0.14	0.24	0.08	0.09	0.01	0.22	nd	0.12	0.31	0.12	0.24	0.16	0.19
Yb	0.87	1.35	0.43	0.67	0.05	1.28	1.13	0.73	2.06	0.87	1.25	1.03	1.13
Lu	0.12	0.19	0.07	0.09	0.01	0.21	0.16	0.11	0.31	0.13	0.19	0.17	0.19
Hf	0.66	0.76	2.17	0.56	2.09	3.45	3.2	1.93	2.31	0.73	2.56	4.52	2.12
Ta	0.24	0.4	1.06	0.24	0.31	1.25	0.49	0.46	n.a.	n.a.	5.32	1.15	0.59
Th	0.25	0.09	1.39	0.65	0.1	13.2	9.58	6.75	n.a.	n.a.	2.97	6.1	3.77
U	0.06	0.04	0.41	0.14	0.09	1.71	2.17	0.72	0.17	2.71	0.66	1.08	1.03
$(La/Yb)_N$	7	5	21	11	53	31	21	22	0.82	1.4	18	19	11
Eu/Eu*	1.04	1.1	1.97	1.04	1.25	0.85	0.84	1.26	1.06	0.98	0.94	0.97	0.93
Rb/Sr	0.069	<0.01	0.03	0.034	0.02	0.09	0.07	0.059	9.19	4.14	0.03	0.25	<0.01

Note: See Tables 1 and 3 for rock names, n.a. means not analyzed.

elements and LREE demonstrate their similarities with sanukitoids.

The Shevchenkovskii Complex consists of tonalites and trondhjemites of the low-Al type, according to (Barker and Arth, 1976): 14–15 wt % Al_2O_3. However, their al = Al_2O_3/(FeO + MgO) ratio places them among highly aluminous rocks. They typically show Na_2O/K_2O ratios of >4; low, as in most tonalites (Martin, 1994), Rb concentrations; moderate Sr contents; and correspondingly, low Rb/Sr ratios. The REE, Th, and Nb concentrations of these rocks are very low (Table 2, Fig. 4b), but the degrees of LREE and HREE fractionation $(La/Yb)_N = 50$, as is characteristic of TTG and is notably different from the rocks of the Obitochnen Complex.

The North Obitochnen Massif, which is dominated by quartz syenites, shows certain mineralogical and geochemical differences: the rocks of this massif differ from the acid rocks of the Obitochnen complex and Osipenkovskii Massif in having higher concentrations of K, Mg, Ti, lithophile elements, and REE (Tables 1, 2; Fig. 4b).

Hence, the plutonic rocks of the Saltychan anticlinorium compose a series, according to an increase in their alkalinity and the degree of their enrichment in lithophile elements, from (1) gabbro, diorites, and granodiorites of the Obitochnen Complex through (2) quartz monzodiorites and quartz syenites of the Osipenkovskii Massif to (3) quartz diorites–quartz syenites of the North Obitochnen Massif. According to their high mg# and enrichment in lithophile elements, the latter two groups may be classed with sanukitoids.

ISOTOPIC AGE OF ROCKS COMPOSING THE AZOV TERRANE

Methods

U–Pb method. Various metamorphic and magmatic rocks from the western Azov domain of the Ukrainian Shield were dated by the U–Pb method on accessory zircons. The zircons were separated from 10- to 15-kg samples, following conventional techniques that involved a combination of magnetic separation and separation in bromoform at the Institute of Geochemistry, Mineralogy, and Ore Genesis, National Academy of Sciences of Ukraine. The morphology and inner structures of zircon crystals were examined in transmitted and incident light. The inner structure of the crystals was also examined by cathodoluminescence.

The isotopic dating of the zircons was conducted by the U–Th–Pb spot technique on a CAMECA 1270 ion probe, NORDSIM, at the Swedish Museum of Natural History in Stockholm. The examined zircon crystals and a standard zircon contained in the same epoxy pellet were polished until their cores were exposed. The inner structures of the crystals were preparatorily examined by cathodoluminescence. Before the analysis, the pellet was sputter-coated with gold. The primary ion beam consisted of O_2^-, which affected an ellipsoidal area 25 × 40 μm at the crystal. The secondary ions were analyzed at a resolution of 5600, which made it possible to discriminate between all of the required atomic masses. The method was described in much detail in (Whitehouse et al., 1997, 1999). The Pb isotopic composition and the U–Pb isotopic ratios were measured accurate to 0.1–0.3% and 1–3%, respectively.

Sm–Nd isotopic method. Sm and Nd isotopic compositions were measured as ion currents of metals on a Finnigan MAT-261 eight-collector mass spectrometer in static mode. Sm and Nd were separated by the conventional technique similar to that described in (Richard et al., 1976). The samples were decomposed in HF and HNO_3 and spiked with a ^{150}Nd and ^{149}Sm tracer. Sm was separated from Nd in two stages: first, all REE were separated in ion-exchange columns, and then Sm and Nd were obtained in columns with HDEHP-covered Teflon powder. The measured $^{143}Nd/^{144}Nd$ ratios were normalized to $^{148}Nd/^{144}Nd = 0.24157$. The Sm and Nd concentrations were determined accurate to ±0.5% (2σ), and the $^{147}Sm/^{144}Nd$ and $^{143}Nd/^{144}Nd$ ratios were determined accurate to ±0.5 and ±0.005% (2σ), respectively. The blanks were 0.05 ng for Sm and 0.1 ng for Nd. The weighted mean $^{143}Nd/^{144}Nd$ ratio in the La Jolla standard during the experiment was 0.511860 ± 12 (2σ).

The $\varepsilon_{Nd}(T)$ were calculated using modern $^{143}Nd/^{144}Nd = 0.512638$ and $^{147}Sm/^{144}Nd = 0.1967$ values for CHUR (Jacobsen and Wasserburg, 1984). The model $T_{Nd}(DM)$ age values were calculated in compliance with the model (DePaolo, 1981), in which the Nd isotopic composition of the depleted mantle evolved according to the formula $\varepsilon_{Nd}(T) = 0.25T^2 - 3T + 8.5$ (where T is in Ga) over the time span from 4.55 Ga to the present, and $\varepsilon_{Nd}(0)) = +8.5$.

U–Pb zircon dating

Intrusive rocks. The dated intrusive rocks were sampled in the Saltychan anticlinorium and southeast of it (Osipenkovskii Massif, Fig. 1). Figure 5 shows cathodoluminescence images of zircon crystals, and Fig. 6 presents a concordia diagram based on the U–Pb isotopic study of these zircons.

Zircons in gabbro from the Elenovskii Massif (sample 2126, mg# = 0.57) are columnar and log-shaped, as is typical of gabbro (Fig. 5a). Their U concentrations are low (66–180 ppm), and the U/Th ratios are high, close to 1 (Table 1), which is typical of zircon form mafic rocks. Their age is 2914 ± 7 Ma (Fig. 6a). Another sample of Fe-richer gabbro from the same massif (sample 2117, mg# = 0.48) contains both columnar and short-prismatic zircons (Fig. 5b). They contain much more U (250–560 ppm) and have relatively high Th/U ratios (0.5–0.9). Their isotopic ages are strongly discordant. The upper-intercept age of these zircons is equal to 2909 ± 17 Ma (Fig. 6b). Gabbro from the East Eliseevskii Massif (sample 2104, mg# = 0.45) contains

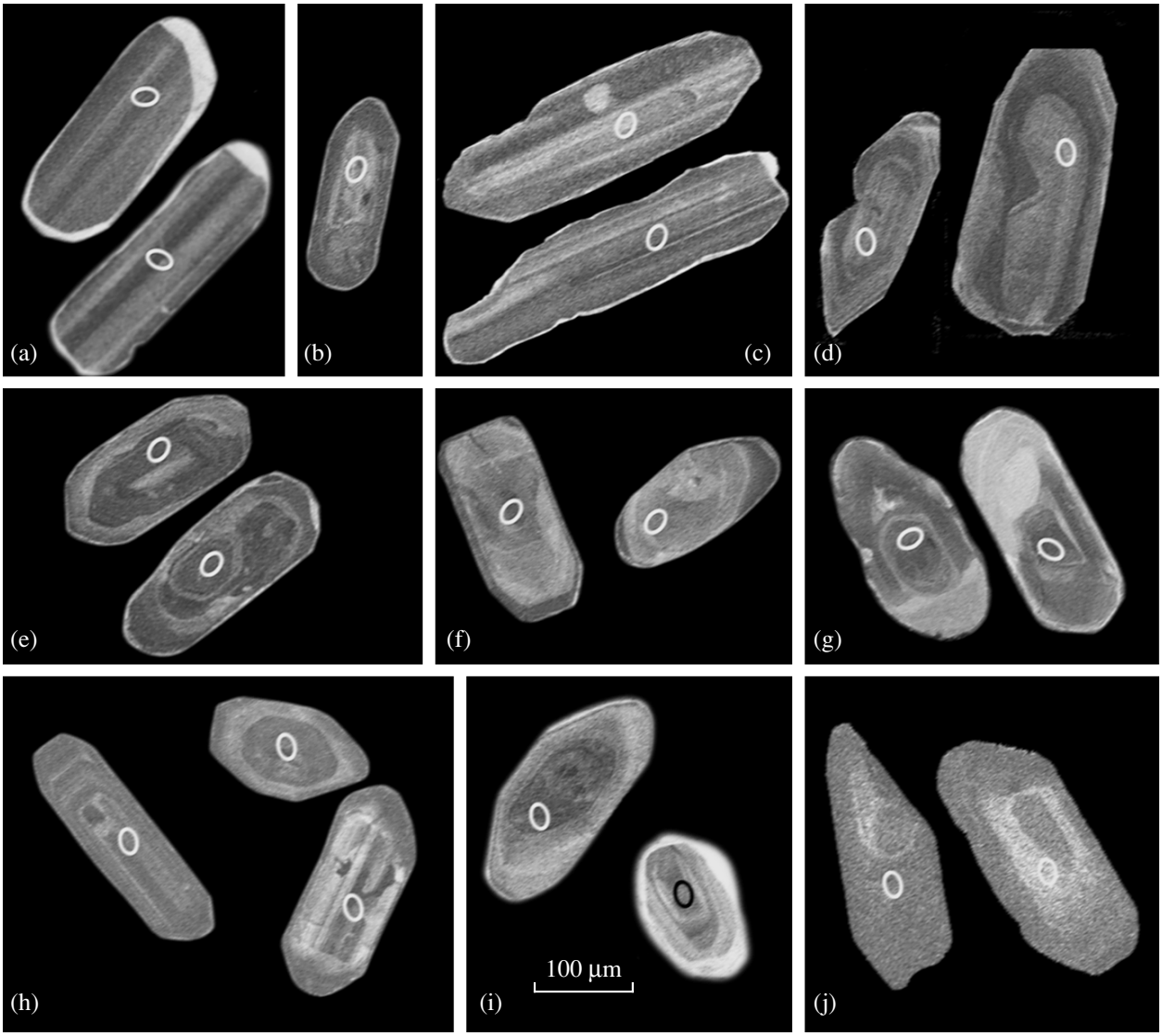

Fig. 5. Cathodoluminescence images of zircon crystals from intrusive rocks from the Azov territory: (a) sample 2126; (b) sample 2117; (c) sample 2104; (d) sample 2155; (e) sample 2176; (f) sample 2188; (g) sample 2194; (h) sample 2127; (i) sample 2122; (j) sample 2153.

columnar and log-shaped zircons (Fig. 5c), which contain as little as 37–60 ppm U, except a single grain that contained 190 ppm U, at a high Th/U ratio of up to 1.33. The isotopic age of the zircons is 2920 ± 13 Ma (Fig. 6c). Thus, two age values of gabbro with different mg# from two massifs are equal (within the analytical error).

Quartz diorite from the Central Obitochnen Massif (sample 2155, mg# = 0.58) contains prismatic, weakly zonal zircons (Fig. 5d) with moderate U concentrations (68–240 ppm) and Th/U ratios from 0.5 to 0.6. The isotopic ages of these zircons are close to concordant and are 2925 ± 8 Ma (Fig. 6d).

Tonalite from the Saltychan Massif (sample 2176, mg# = 0.41) contains prismatic zonal zircons, some of which possess discernible cores (Fig. 5e). The zircons have relatively low U concentrations (72–240 ppm) and low Th/U ratios in the cores and somewhat higher (0.7) in zonal crystals. The isotopic age of the zonal crystals is 2907 ± 5 Ma, and the concordant age (Ludwig, 1999) of the cores is 2940 ± 5 Ma (Fig. 6e).

Vein trondhjemites from the Shevchenkovskii Complex (sample 2188) contain prismatic zircons, whose crystals are either zonal or homogeneous (Fig. 5f). Their U concentrations are very low (51–92 ppm), and the Th/U ratio is lower than 0.6. The age of these zircons is 2941 ± 9 Ma (Fig. 6f).

A dike of mafic high-Mg hornblendite (sample 2194) contains large prismatic, weakly zonal zircons (Fig. 5g). Their U concentrations are very low (49–84 ppm), and the Th/U ratio is high, close to 1. The

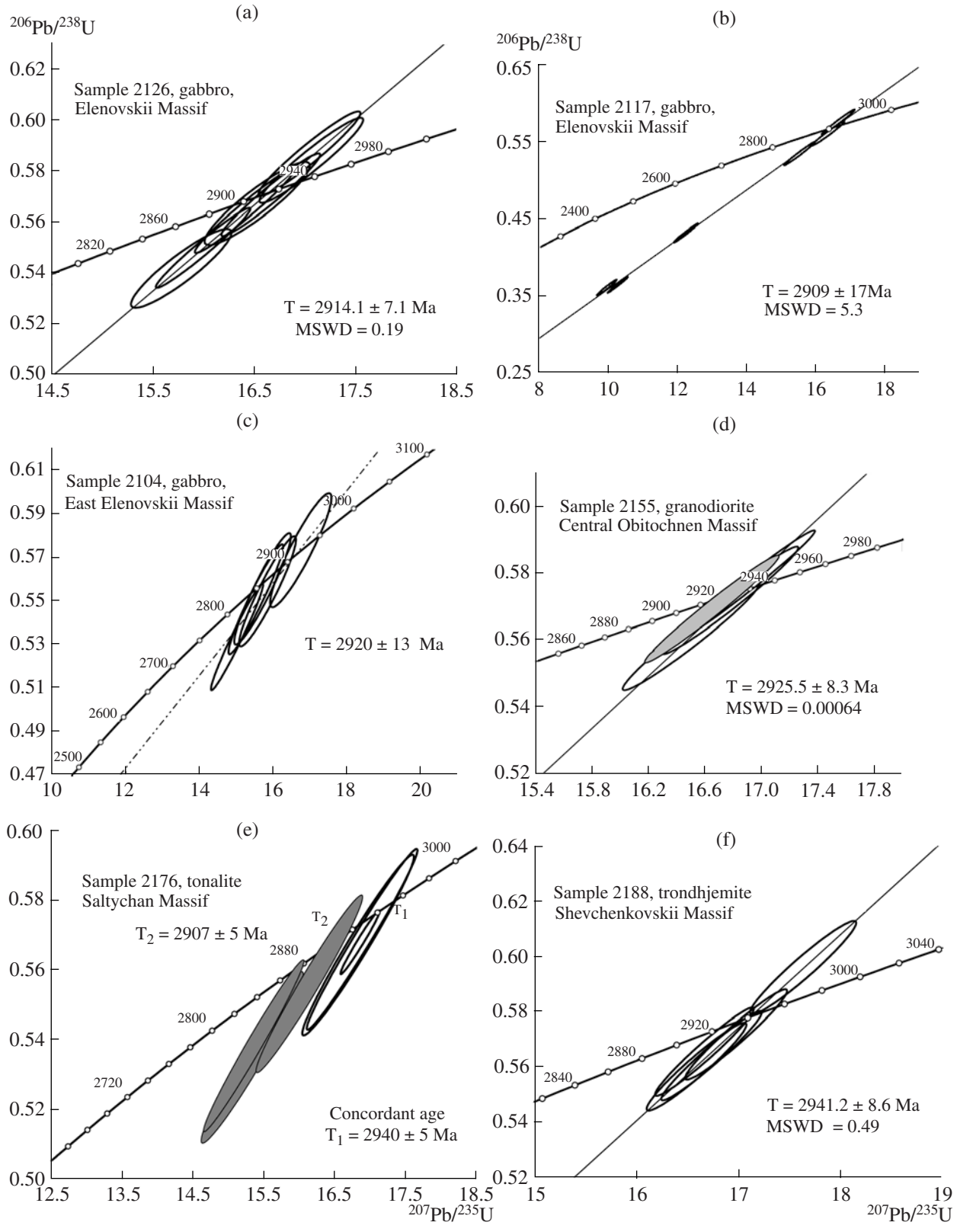

Fig. 6. Concordia plots for zircons from intrusive rocks from the Azov area.

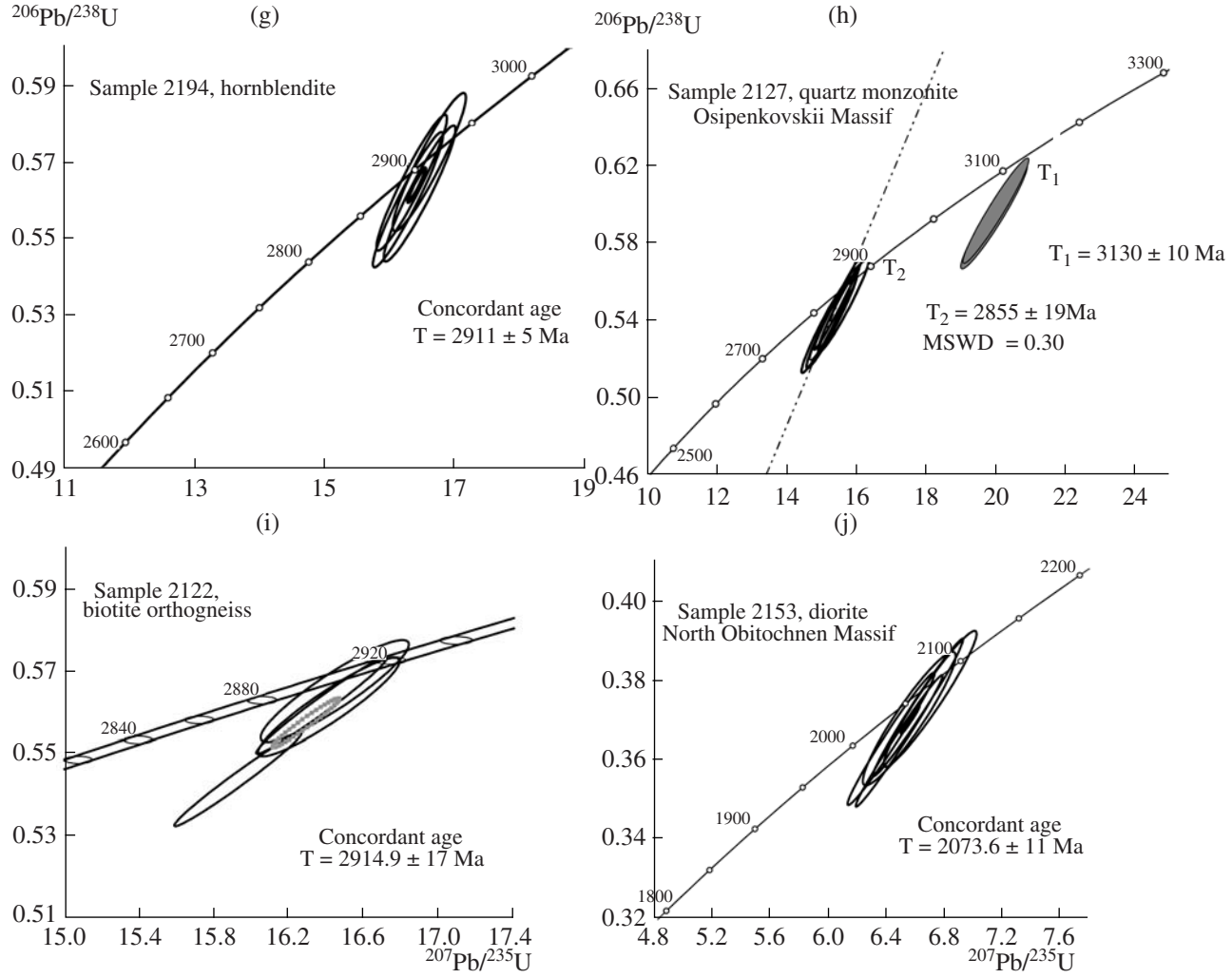

Fig. 6. (Contd.).

isotopic ages are practically concordant and close to 2908 ± 5 Ma (Fig. 6g).

A quartz monzodiorite intrusion in the Osipenkovskii Massif (sample 2127, mg# = 0.60) in the peripheral portion of the Saltychan anticlinorium hosts xenoliths of sheared metabasalts from the Sorokinskii greenstone belt. Zircons from the rocks are prismatic, euhedral, zonal, and sometimes contain discernible cores (Fig. 5h). The U concentrations are low (37–100 ppm, 196 ppm in one grain), the Th/U ratio in zircon cores is very high: up to 1.44. The isotopic age is 2855 ± 19 Ma. The cores of these zircons were determined to contain a more ancient component with an age of 3130 Ma (Fig. 6h).

Biotite gneiss (sample 2122) from a thin gneiss layer in amphibolites exposed in the Mogila Zelenaya quarry contains prismatic two-phase zircons. Their inner parts are zonal and are surrounded by transparent low-U zones. U is unevenly distributed in the crystals and ranges from 30 to 700 ppm, with the Th/U ratio correspondingly varying. The age of the inner zonal parts of these crystals is 2920 Ma (Fig. 6i). As was mentioned above, structural observations indicate that the protolith of this gneiss layer could be a trondhjemite vein, a conclusion that is corroborated by the obtained age values. Original data were obtained on the North Obitochnen Massif, which is composed of quartz diorites–quartz syenites. Zircons from the quartz diorite (sample 2153, mg# = 0.61) are short-columnar (Fig. 5j), homogeneous, and their U concentrations are relatively high (92–389 ppm) at a Th/U ratio of about 0.5. The isotopic ages are almost concordant and equal to 2073.6 ± 11 Ma (Fig. 6j).

Metamorphic rocks of the West Azov Group. It was interesting to date the early metamorphism of the West Azov Group. For this purpose, we examined zircons separated from metamorphic rocks from the West Azov Group, which were sampled at two exposures of these rocks: in the Saltychan anticlinorium (samples

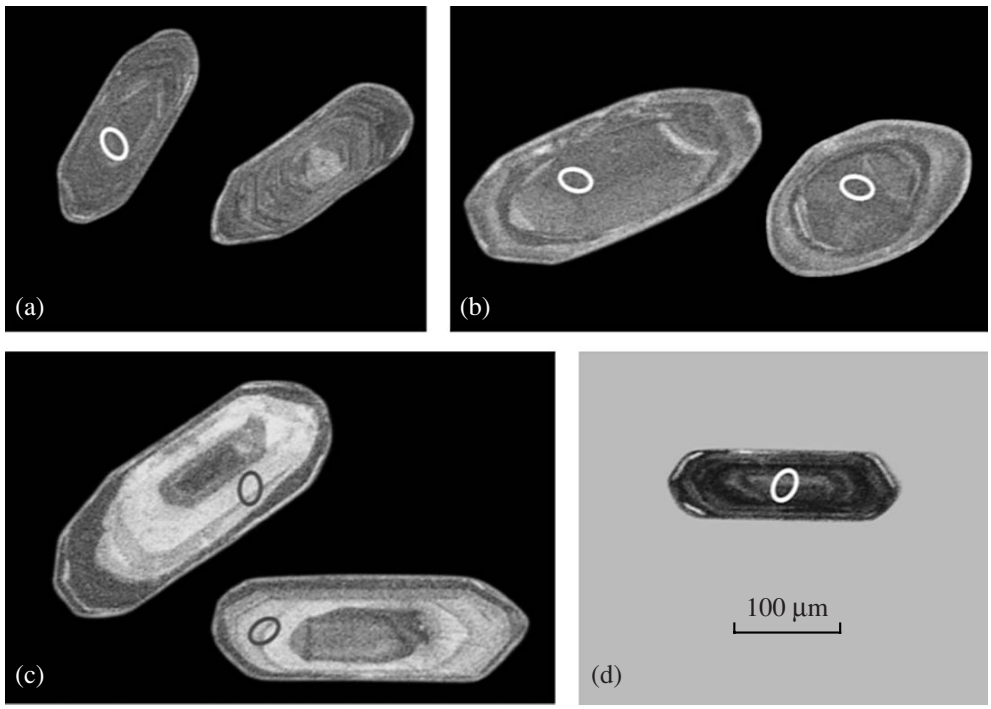

Fig. 7. Cathodoluminescence images of zircon crystals from the host rocks of the West Azov Group: (a) sample 2005; (b) sample 2171; (c) sample 84-102; (d) sample 2197.

2005 and 2117) and in the northern part of our study area (samples 84-102 and 2197) (Fig. 1).

Amphibole–biotite gneiss (sample 2005) from the northwestern part of the Saltychan anticlinorium, not far from the Mogila Zelenaya quarry (Fig. 1) contains elongated-prismatic zonal zircons. Such zoning is typical of both magmatic zircon grains and crystals of this mineral of metamorphic genesis that grew in the presence of fluid (Fig. 7a). The U concentrations are moderate, and the isotopic ages are mostly discordant. The upper intercept of the discordia and concordia corresponds to an age of 3076 ± 35 Ma (Fig. 8a).

Biotite plagiogneiss (sample 2171) from the central part of the eastern margin of the Saltychan anticlinorium (Fig. 1) contains two-phase zircons. The central parts of their grains are fairly rich in U and are surrounded by zones poorer in U. The upper-intercept age of the central parts of the crystals is 3122 ± 16 Ma (Figs. 7b, 8b).

Amphibole–biotite gneiss (sample 84-102) sampled from the West Azov Group in the northern part of our study area bears prismatic, weakly zonal zircon crystals poor in U (40–50 ppm). The crystals are surrounded by thin darker high-U outermost zones (Fig. 7c). The upper intercept of the discordia and concordia for the central parts of these crystals yields an age of 3014 ± 22 Ma (Fig. 8c).

Amphibolite (sample 2197) was taken from a layer intercalating with amphibole–biotite and biotite gneisses in the vicinity of sampling site 84-102. Zircons in the amphibolite are prismatic, weakly zonal, and have a metamorphic genesis (Fig. 7d). The U concentrations in these zircons are fairly high, which accounts for the often discordant U–Pb age of these zircons. The upper-intercept age corresponds to 3024 ± 4 Ma (Fig. 8d).

Our isotopic data imply that early metamorphism in the rocks of the West Azov Group took place at 3120–3000 Ma.

Nd isotopic composition

Nd isotopic composition was determined for samples of the Archean and Proterozoic intrusive rocks (Table 4). The Archean intrusions (Central Obitochnen, Elenovsii, Krymsii, Uspenovsii, and Osipenkovsii), which were emplaced within the age span of 2.85–2.92 Ga, are characterized by $\varepsilon_{Nd}(T)$ values close to zero and $T_{Nd}(DM)$ close to 3 Ga. Rocks from the Saltychan Massif have higher $\varepsilon_{Nd}(T) = 1.2$ and a model age $T_{Nd}(DM)$ close to the crystallization age (2980 and 2940 Ma, respectively). The Proterozoic intrusions (North Obitochnen and Kamyshevatskii massifs) have lower $\varepsilon_{Nd}(T)$ values from –3.3…–3.4 to –4.1 at $T_{Nd}(DM)$ ~ 2.6 Ga (Fig. 9).

The Nd isotopic composition of the Archean rocks may be indicative of (1) a time gap separating the enrichment of the mantle source and its subsequent melting and (2) the effect of older crustal material on the Nd isotopic composition of the magma. Our rocks

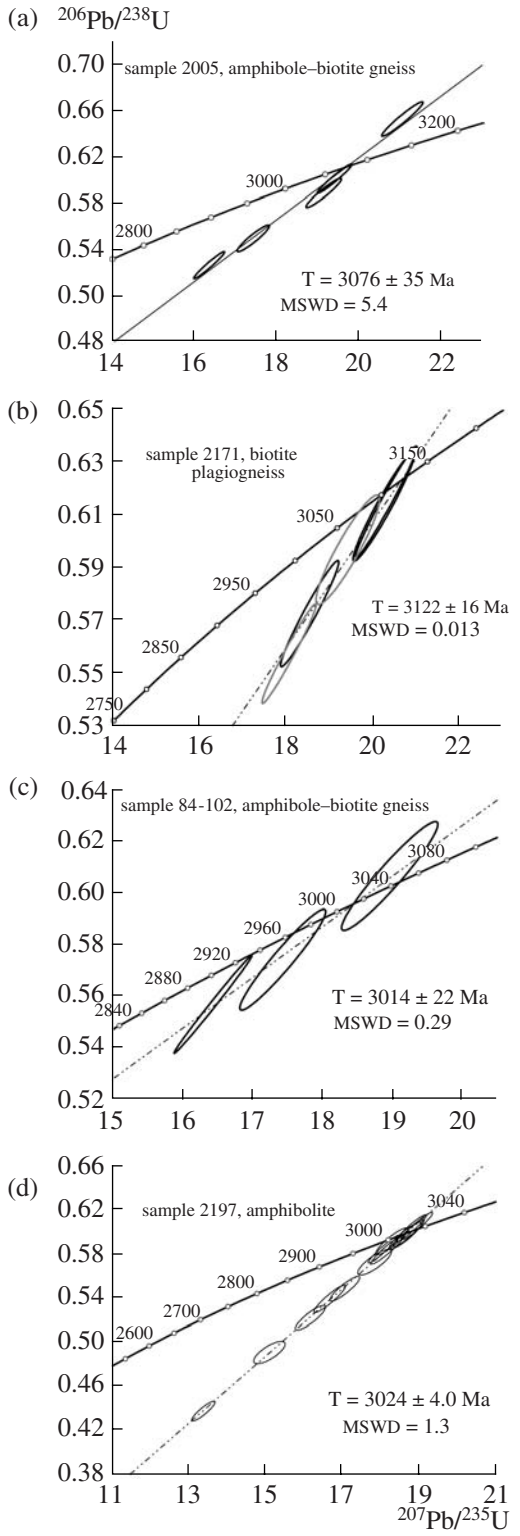

Fig. 8. Concordia diagrams for zircons from the host rocks of the West Azov Group.

have moderately high REE concentrations (Nd < 40 ppm), which are comparable with the REE concentrations of the host metamorphic rocks and the rocks of

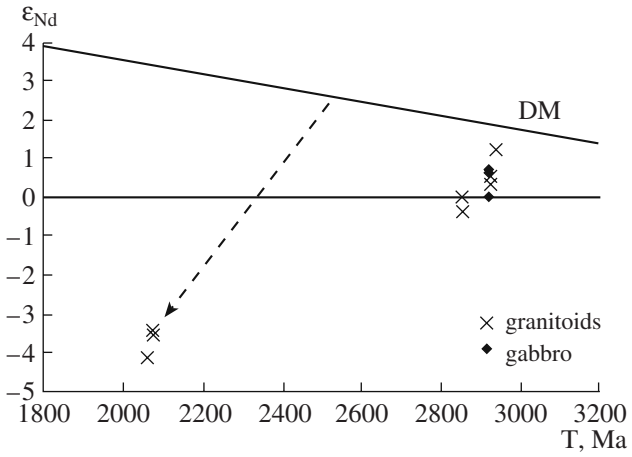

Fig. 9. ε_{Nd}–T diagram for intrusive rocks of the Azov territory. The arrow indicates the evolution of the Nd isotopic composition of Proterozoic quartz monzonite (sample 2053).

the TTG series. Thus, the isotopic system of the intrusions could be susceptible to contamination with ancient crustal material. With regard for the facts and considerations presented above, both factors could affect the Nd isotopic composition of the Archean intrusions.

Sm–Nd data on the Saltychan Massif testify to the minimum involvement of crustal material and/or the minimum age gap between the enrichment of the source and its melting. Negative $\varepsilon_{Nd}(T)$ values of the Proterozoic intrusions (North Obitochnen and Kamyshevatskii massifs) suggest that they were derived from a source with a long prehistory. The model age $T_{Nd}(DM)$ of approximately 2.6 Ga could correspond to the enrichment timing of the mantle source.

DISCUSSION

The Saltychan anticlinorium hosts a number of successively produced groups of metamorphic and intrusion rocks.

The quartz–feldspathic gneisses and amphibolites attributed to the West Azov Group are widespread throughout the whole territory of the West Azov domain. Our isotopic data indicate that the early metamorphism of rocks of the West Azov Group occurred at 3120–3000 Ma. Neither accessory zircons from the gneisses nor Sm–Nd dates yielded ages older than 3120 Ma.

The emplacement of the Obitochnen intrusive complex (gabbro and granitoids of both normal and elevated mg#) in the Saltychan magmatic province took place within a narrow time span from 2940 to 2910 Ma. An analogous age was yielded by the hornblendites (2908 ± 5 Ma).

Table 3. Isotopic data on sanukitoids and their host rocks in the Azov megablock

Sample no. and sampling site	Concentration, ppm			Th/U	$^{206}Pb_{common}$	Isotopic ratios		Age, Ma	Discordance, %
	U	Th	Pb			$^{206}Pb/^{238}U$	$^{207}Pb/^{235}U$	$^{207}Pb/^{206}Pb$	
Elenovskii Massif									
Gabbro (sample 2126)									
2126-1	77	60	64	0.78	0.08	0.5869 ± 109	17.040 ± 319	2909 ± 9	–3
2126-2	181	206	137	1.14	0.05	0.5843 ± 110	17.058 ± 320	2919 ± 10	–2
2126-3	88	66	70	0.75	0.40	0.5505 ± 109	15.992 ± 300	2887 ± 7	4
2126-4	135	119	106	0.88	0.14	0.5674 ± 107	16.525 ± 310	2912 ± 7	1
2126-5	134	128	108	0.95	0.03	0.5645 ± 108	16.400 ± 315	2915 ± 14	1
2126-6	116	93	85	0.80	0.03	0.5708 ± 108	16.659 ± 315	2911 ± 7	0
2126-7	116	96	93	0.83	0.04	0.5420 ± 107	15.776 ± 300	2918 ± 8	5
2126-8	66	40	52	0.61	0.13	0.5922 ± 109	16.958 ± 310	2914 ± 14	–5
Gabbro (sample 2117)									
2117-1	557	453	283	0.81	0.29	0.3623 ± 68	9.966 ± 189	2822 ± 6	34
2117-2	247	121	187	0.49	0.02	0.5622 ± 105	16.368 ± 310	2914 ± 6	2
2117-3	410	304	246	0.74	0.80	0.4329 ± 100	12.254 ± 250	2869 ± 5	22
2117-4	407	291	328	0.72	0.08	0.5771 ± 105	16.658 ± 310	2900 ± 5	–2
2117-5	333	285	257	0.86	0.22	0.5361 ± 100	15.539 ± 290	2907 ± 5	6
Central Obotochnen massif, granodiorite (sample 2155)									
2155-1	109	58	85	0.53	0.03	0.5719 ± 106	16.777 ± 310	2913 ± 6	1
2155-2	135	70	106	0.52	0.03	0.5767 ± 105	16.895 ± 300	2924 ± 5	–1
2155-3	238	127	184	0.53	0.02	0.5694 ± 105	16.610 ± 310	2917 ± 6	1
2155-4	68	39	52	0.57	0.05	0.5610 ± 100	16.495 ± 300	2930 ± 7	3
North Obotochnen massif, diorite (sample 2153)									
2153-2	304	151	144	0.49	0.05	0.3739 ± 70	6.624 ± 120	2077 ± 6	2
2153-3	300	250	150	0.84	0.06	0.3655 ± 69	6.4314 ± 125	2065 ± 6	3
2153-4	123	78	61	0.63	0.06	0.3756 ± 70	6.700 ± 130	2089 ± 10	2
2153-5	268	121	126	0.45	0.03	0.3731 ± 70	6.613 ± 120	2078 ± 6	2
2153-6	92	46	43	0.51	0.05	0.3706 ± 70	6.556 ± 122	2074 ± 12	2
Saltychan Massif, tonalite (sample 2176)									
2176-1	87	50	68	0.57	0.09	0.5685 ± 100	16.818 ± 320	2940 ± 7	2
2176-2	127	71	99	0.56	0.04	0.57018 ± 105	16.875 ± 320	2941 ± 5	1
2176-3	129	63	86	0.49	0.19	0.4912 ± 90	14.258 ± 300	2910 ± 6	4
2176-4	72	52	54	0.72	0.04	0.5365 ± 100	15.327 ± 310	2884 ± 7	4
2176-5	240	184	182	0.76	0.4	0.5398 ± 10	15.346 ± 310	2875 ± 5	4
2176-6	98	69	76	0.70	0.06	0.5576 ± 100	16.132 ± 315	2904 ± 6	2
East Eliseevskii Massif, gabbro (sample 2104)									
2104-1	60	33	47	0.55	0.09	0.5735 ± 107	16.752 ± 335	2920 ± 13	0
2104-2	59	43	45	0.72	0.17	0.5510 ± 100	15.532 ± 302	2862 ± 9	1.4
2104-3	54	50	43	0.91	1.06	0.5577 ± 110	15.715 ± 300	2867 ± 11	1
2104-4	190	252	158	1.33	0.1	0.5337 ± 105	15.021 ± 300	2859 ± 7	4
2104-5	37	29	29	0.77	0.13	0.5546 ± 107	15.849 ± 305	2884 ± 11	1.7
2104-6	52	32	39	0.62	0.23	0.5426 ± 105	15.833 ± 302	2918 ± 10	5

Table 3. (Contd.)

Sample no. and sampling site	Concentration, ppm			Th/U	$^{206}Pb_{common}$	Isotopic ratios		Age, Ma	Discordance, %
	U	Th	Pb			$^{206}Pb/^{238}U$	$^{207}Pb/^{235}U$	$^{207}Pb/^{206}Pb$	
Shevchenkovskii Complex, trondhjemite (sample 2188)									
2188-1	51	20	38	0.40	0.04	0.5602 ± 105	16.588 ± 320	2942 ± 9	3
2188-2	60	27	46	0.44	0.06	0.5719 ± 105	16.976 ± 320	2946 ± 8	1
2188-3	92	52	71	0.57	0.02	0.5642 ± 105	16.735 ± 320	2944 ± 8	2
2188-4	71	34	54	0.48	0.03	0.5657 ± 105	16.666 ± 320	2933 ± 8	2
2188-4a	84	48	68	0.57	0.18	0.5961 ± 105	17.633 ± 320	2940 ± 9	–3.0
Osipenkovskii Massif, quartz monzonite (sample 2127)									
2127-1	96	95	79	0.99	0.02	0.5577 ± 105	15.943 ± 307	2885 ± 7	1.0
2127-2	196	200	160	1.02	0.22	0.5499 ± 105	15.473 ± 305	2859 ± 5	2
2127-3	96	76	74	0.79	0.03	0.5399 ± 105	15.268 ± 300	2867 ± 8	4
2127-4, core	37	17	30	0.41	0.09	0.594 ± 117	19.783 ± 388	3130 ± 9	5
2127-4a, core	43	19	35	0.44	0.08	0.5968 ± 115	19.832 ± 390	3126 ± 8	4
2127-5	66	29	48	0.44	0.04	0.5485 ± 105	15.616 ± 300	2878 ± 9	3
2127-6	59	67	48	1.13	0.06	0.5376 ± 105	15.122 ± 295	2858 ± 8	4
2127-7	79	112	69	1.41	0.06	0.5443 ± 105	15.362 ± 300	2864 ± 7	3
Central Obitochnen Massif, hornblendite (sample 2194)									
2194-1	49	35	35	0.72	0.05	0.5970 ± 85	13.989 ± 185	2807 ± 19	6
2194-10	81	94	69	1.17	0.03	0.5603 ± 85	16.287 ± 220	2912 ± 7	1.9
2194-11	56	39	45	0.70	0.05	0.5701 ± 80	16.614 ± 210	2916 ± 8	0
2194-12	82	99	72	1.20	0.04	0.5647 ± 80	16.344 ± 220	2904 ± 7	0
2194-13	84	85	71	1.00	0.04	0.5619 ± 80	16.467 ± 220	2925 ± 7	2
Eliseevskii Massif, biotite orthogneiss (sample 2122)									
2122-2	255	71	179	0.28	0.34	0.5439 ± 76	15.926 ± 220	2924 ± 4	6
2122-5	400	125	90	0.31	0.19	0.1668 ± 32	4.813 ± 90	2899 ± 4	70
2122-6	139	79	107	0.56	0.02	0.562 ± 80	16.372 ± 220	2915 ± 4	2
2122-7	33	60	32	1.82	0.08	0.5616 ± 80	16.411 ± 230	2920 ± 9	2
2122-8	29	17	23	0.56	0.06	0.5655 ± 80	16.443 ± 230	2912 ± 10	1
2122-9	698	133	96	0.19		0.1044 ± 25	3.033 ± 80	2911 ± 6	80
2122-10	76	41	60	0.54	0.04	0.5842 ± 82	17.228 ± 240	2935 ± 6	–1
West Azov Group Amphibole–biotite gneiss (sample 2005)									
2005-1	178	135	152	0.76	0.05	0.5891 ± 88	19.124 ± 280	3089 ± 8	4
2005-2	181	117	166	0.65	0.18	0.6529 ± 100	21.031 ± 300	3076 ± 7	7
2005-3	358	200	251	0.35	0.03	0.5269 ± 80	16.347 ± 240	3017 ± 6	12
2005-4	108	59	90	0.56	0.12	0.6013 ± 90	19.386 ± 280	3078 ± 5	2
2005-5	272	123	203	0.43	0.15	0.55005 ± 75	17.417 ± 250	3049 ± 8	9
Plagiomigmatite (sample 2171)									
2171-1	161	167	151	1.04	0.03	0.6149 ± 86	20.295 ± 285	3116 ± 4	1
2171-2	178	170	164	0.96	0.01	0.6132 ± 85	20.238 ± 285	3116 ± 6	1
2171-3	45	40	39	0.88	0.06	0.5967 ± 80	19.407 ± 270	3092 ± 10	3
2171-4	148	72	117	0.48	0.06	0.5726 ± 80	18.527 ± 270	3084 ± 6	7
2171-4a	66	75	47	1.14	0.81	0.4762 ± 67	14.167 ± 200	2864 ± 10	9
2171-6	203	69	150	0.34	0.27	0.5574 ± 75	18.050 ± 250	3085 ± 5	9
2171-7	609	23	356	0.04	0.22	0.4582 ± 60	12.837 ± 200	2949 ± 6	18

Table 3. (Contd.)

Sample no. and sampling site	Concentration, ppm			Th/U	$^{206}Pb_{common}$	Isotopic ratios		Age, Ma	Discordance, %
	U	Th	Pb			$^{206}Pb/^{238}U$	$^{207}Pb/^{235}U$	$^{207}Pb/^{206}Pb$	
Amphibole–biotite gneiss (sample 84-102)									
84102-01	1017	159	713	0.156	0.05	0.5569 ± 70	16.415 ± 240	2934 ± 2	0.7
84102-02	54	31	43	0.568	0.05	0.5741 ± 70	17.415 ± 220	2980 ± 7	2.3
84102-03	41	26	34	0.629	0.05	0.6064 ± 80	18.948 ± 240	3028 ± 7	–1.1
84102-04	227	78	130	0.345	0.05	0.4342 ± 60	12.847 ± 200	2940 ± 6	22.2
Amphibolite (sample 2197)									
2197-1	351	85	150	0.231	1.69	0.3304 ± 33	8.597 ± 90	2731 ± 9	35.0
2791-2	227	129	170	0.551	0.09	0.5392 ± 54	16.662 ± 150	3010 ± 6	7.0
2791-3	405	166	324	0.378	0.01	0.6032 ± 60	18.784 ± 150	3023 ± 4	–0.8
2791-4	306	275	270	0.869	0.04	0.6053 ± 60	18.943 ± 150	3031 ± 4	2.0
2791-5	465	144	355	0.294	0.04	0.5844 ± 58	18.075 ± 150	3012 ± 4	2.4
2791-6	329	115	253	0.325	0.02	0.5840 ± 58	18.177 ± 150	3022 ± 5	0.7
2791-7	257	128	206	0.473	0.01	0.5914 ± 59	18.287 ± 150	3012 ± 7	0.8
2791-8	187	286	145	0.648	0.22	0.5484 ± 54	17.058 ± 140	3021 ± 7	8.0
2791-9	814	979	586	0.792	0.21	0.4881 ± 48	14.642 ± 130	2962 ± 6	16.0
2791-10	290	263	225	0.850	0.70	0.5222 ± 52	16.159 ± 150	3013 ± 8	12
2791-11	155	113	101	0.303	0.20	0.4909 ± 49	15.086 ± 150	3002 ± 12	17
2791-12	229	100	181	0.384	0.03	0.5965 ± 59	18.636 ± 150	3028 ± 6	0.5
2791-13	479	468	421	0.895	0.02	0.5986 ± 60	18.725 ± 150	3030 ± 4	0.2
2791-14	218	159	175	0.626	0.19	0.5724 ± 60	17.835 ± 160	3024 ± 9	4.0
2791-15	340	198	203	0.393	0.08	0.4377 ± 45	13.359 ± 120	2991 ± 6	25.0

The Osipenkovskii sanukitoid monzodiorite–monzonite intrusion is younger: its age corresponds to 2855 ± 19 Ma.

The Proterozoic was marked in the Azov territory by compositionally diverse magmatism, whose products range from lamproites and carbonatites to lamprophyres, granites, and pegmatites. According to our data, the North Obitochnen sanukitoid monzonite–syenite intrusion in the Saltychan anticlinorium has a concordant zircon age of 2074 ± 11 Ma. Data on the Nd isotopic composition testify that the magma was derived from Archean intrusive rocks (Fig. 9). The lamprophyre dikes exposed in the Elenovskii quarry seem to be also emplaced in the Proterozoic, as follows form the Nd model ages of these rocks: $T_{Nd}(DM)$ = 2100–2200 Ma.

The synchronous emplacement of melts derived from a mantle and a crustal source suggests the thermal and/or decompressional melting of the lithosphere at various depths under the effect of an ascending plume.

In the West Azov province, Late Archean gabbro–granitoid intrusions were emplaced into metamorphosed, tectonized, and migmatized rocks of the West Azov Group. A fact important for understanding the tectonic environment of the Late Archean magmatism is the discovery of the age gap (>70 Ma long) between the regional metamorphism of the West Azov Group and the subsequent intrusive activity. This implies that the initiation of the magmatism was not related to the orogenic processes that ended with the metamorphism and migmatization of the West Azov Group. The most probable thermal source that provided heat for mantle melting and the derivation of the parental magmas of the Obitochnen Complex was the ascent of hot melts of a plume. The simultaneous emplacement of melts with distinct geochemical characteristics provides further arguments in support of the idea that the melting processes were related to the ascent of a plume, because the basic melts could be derived from both heterogeneous lithospheric mantle and the melts of the plume, which caused a more magnesian composition of the basite melts.

The parental melts of the granitoids were most probably of diorite composition and were produced by the partial melting of a H_2O-bearing peridotite. The possibility of this processes has been demonstrated in (Kushiro, 1972). Compositional variations within an intrusion were controlled by fractional crystallization. The fact that zircons from the Osipenkovskii Massif have cores with an age of approximately 3130 Ma suggests the involvement of younger material in the gene-

Table 4. Data on the Sm–Nd isotopic system in intrusion rocks from the Azov megablock, Ukrainian Shield

Sample	Rock	Sm, ppm	Nd, ppm	Sm/Nd	$^{147}Sm/^{144}Nd$	$^{143}Nd/^{144}Nd$	±2σ	$\varepsilon_{Nd}(0)$	$\varepsilon_{Nd}(T)$	$f_{Sm/Nd}$	T_{Zr}	$T_{Nd}(DM)$
Elenovskii Massif												
2104	gabbro	4.18	21.82	0.19	0.1158	0.511076	9	−30.5	0.0	−0.411	2920	3077
7/7-02	tonalite	0.52	4.25	0.12	0.0737	0.510305	9	−45.5		−0.625		2982
Uspenovski Massif												
2172	gabbro	7.63	41.82	0.18	0.1103	0.511003	8	−31.9	0.6	−0.439	2920	3017
Krymskii Massif												
4536	gabbro	2.46	15.46	0.16	0.0963	0.510736	12	−37.1	0.7	−0.510	2920	3001
Central Obitochnen Massif												
5-02	quartz diorite	2.94	15.88	0.19	0.1118	0.511016	10	−31.6	0.3	−0.432	2925	3044
2154	gabbro	0.82	3.38	0.24	0.1461	0.511688	13	−18.5	0.5	−0.257	2925	3087
Saltychan Massif												
2176	tonalite	0.77	5.44	0.14	0.0852	0.510533	9	−41.1	1.2	−0.567	2940	2980
Osipenkovskii Massif												
12/3	quartz syenite	3.7	23.6	0.16	0.0948	0.510720	6	−37.4	0.0	−0.518	2855	2983
13/2	quartz syenite	6.71	42.5	0.16	0.0955	0.510709	8	−37.6	−0.4	−0.514	2855	3016
Kamyshevatskii Massif												
2156	quartz monzonite	7.37	42.47	0.17	0.1049	0.511186	8	−28.3	−4.1	−0.467	2060	2595
North Obitochnen Massif												
6-02	quartz monzonite	4.6	26.3	0.17	0.1057	0.511215	6	−27.8	−3.5	−0.463	2073	2573
2153	quartz monzonite	4.5	25.35	0.18	0.1074	0.511248	11	−27.1	−3.4	−0.454	2073	2567
Dike Complex												
8/6-02	lamprophyre	3.33	17.6	0.19	0.1145	0.511591	7	−20.4		−0.418		2216
7/1-02	fine-grained gabbro	8.04	63.05	0.13	0.0771	0.511133	9	−29.4		−0.608		2116

Note: $f_{Sm/Nd}$ is the $^{147}Sm/^{144}Nd$ enrichment coefficient in the sample relative to CHUR, T_{Zr}–U-Pb is the zircon isotopic age.

sis of the parental melt of this massif, which is consistent with the Nd isotopic age of the rocks.

The comparison of the compositions that have similar SiO_2 concentrations and were produced at approximately 2920 Ma (Central Obitochnen Massif), 2850 Ma (Osipenkovskii Massif), and approximately 2000 Ma (North Obitochnen Massif) demonstrates that the concentrations of alkalis and some other lithophile elements increased with time, and this could not result from the different degrees of melting of a source of relatively homogeneous composition but likely reflects the systematic enrichment of the mantle domains from which the melts were derived.

The Nd isotopic composition of the rocks shows that most intrusions of the Saltychan magmatic province were derived from slightly enriched mantle that was much less enriched than younger (2.74–2.69 Ga) sanukitoids in Canada (Stern and Hanson, 1991) and Karelia (Lobach-Zhuchenko et al., 2005). The enrichment of the mantle in LREE took place at about 3000 Ma, which corresponds to the metamorphic age of the supracrustal rocks. This process was separated from the derivation and emplacement of the sanukitoids and calc–alkaline melts by a time interval of 80–120 Ma.

PRINCIPAL CONCLUSIONS

The Saltychan magmatic province recognized and studied in the Azov domain of the Ukrainian Shield was produced at 2.94–2.91 Ga and provides an example of a continental province of within-plate magmatism. The rocks hosting this province (West Azov Group) are dated at 3120–3000 Ma. Our isotopic data reveal a time gap of >80 Ma between metamorphic processes in the host rocks of this magmatic province and the emplacement of itself.

A correlation between endogenic processes in three Archean domains of the shield [Dnestr–Bug (Podolian), Middle Dnepr, and Azov] (Table 5) demonstrates the unique character of the Azov domain, in which magmatism occurred at 2.94–2.91 Ga.

Isotopic and geochemical data testify that most of the intrusions were produced by melts derived from mantle material.

Table 5. Correlation of endogenic processes in the Azov, Dnepr, and Podolian blocks of the Ukrainian Shield

Age, Ma	Azov domain	Dnepr domain	Podolian domain
2800	Metamorphism to the amphibolite facies, migmatization of the West Azov Group, TTG (1, 2)	Late- and postkinematic granites (2)	Metamorphism to the granulite and amphibolite facies (7)
2850			
2900	Saltychan magmatic province (Obitochnen gabbro–diorite complex)		
2950		Intrusions of high-Mg diorites (6)	
3000	Metamorphism of the West Azov Group to the granulite and amphibolite facies (1)	Metamorphism to the amphibolite facies, TTG intrusions	
3050		Volcano–sedimentary series of greenstone belts (3, 5)	
3100		Tonalite intrusions	
3150		Protolith of the Aul'skaya Group (3, 5)	
3200			
3250			
3300			
3350	Metamorphism, enderbites,, Orekhovo–Pavlograd tectonic zone (2)		Enderbites (4, 7)
3400			
3450			
3500			
3550			
3600			
3650	Apopyroxenites, tonalites, Orekhovo–Pavlograd tectonic zone (2)		Tonalites (4, 7)
3700			
3750			

Note: references: (1) this publication; (2) (Bibikova et al., 1990); (3) (Shcherbak et al., 2005); (4) (Claesson et al., 2006); (5) (Samsonov et al., 1996); (6) (Bibikova, unpublished data); (7) Bibikova et al., 1982).

We distinguished the North Obitochnen sanukitoid massif of Proterozoic age (2074 ± 11 Ma), which demonstrates two stages of similar magmatism in the Saltychan anticlinorium and highlights the diversity of Proterozoic mantle magmatism in the Azov megablock.

The results of our research lead to a significant revision of the evolutionary history of the Azov domain. Its inner structure and evolution over the time span from the Mesoarchean to Paleoproterozoic make this domain remarkably different from the Middle Dnepr and Podolian domains and led us to regard the Azov domain as an individual terrane.

ACKNOWLEDGMENTS

The authors thank M. Whitehouse (Swedish Museum of Natural History) for the possibility of carrying out isotopic analyses on a secondary-ion mass spectrometer in Stockholm. L. Il'insky (Swedish Museum of Natural History) is thanked for help with ion-microprobe analyses. The authors also thank the reviewers, A.V. Samsonov and S.P. Korikovsky (Institute of the Geology of Ore Deposits, Petrography, Mineralogy, and Geochemistry, Russian Academy of Sciences), for numerous valuable comments that allowed us to notably improve the manuscript. This study was financially supported by the Russian Foundation for Basic Research (project nos. 03-05-65051 and 06-05-64458) and Programs 4 and 8 of the Division of Earth Science of the Russian Academy of Sciences and was carried out within the scope of NORDSIM Project, Stockholm, Sweden.

REFERENCES

1. G. V. Artemenko, "Geochronological Correlation of Volcanism and Granitoid Magmatism of the Southeastern Ukrainian Shield and Kursk magnetic Anomaly," Geokhimiya Rudoobrazovanie, No. 21, 129–154 (1995).
2. G. V. Artemenko, E. A. Tatarinova, B. V. Borodynya, and T. I. Dovbush, "Age of the Intrusion of the Saltychan Antiklinorium," Mineral. Zh., No. 2/3, 93–96 (2003).
3. G. V. Artemenko, E. A. Tatarinova, V. A. Shpyl'chak, et al., "U–Pb Age of the Tonalite–Granodiorite Associa-

tion of the Gaichurskii Block (Western Azov Region)," Mineral. Zh. **24** (1), 28–33 (2002).

4. E. V. Bibikova, *Uranium–Lead Geochronology of the Early Evolutionary Stages of Shields* (Nauka, Moscow, 1989) [in Russian].
5. E. V. Bibikova, I. M. Lesnaya, and T. V. Gracheva, "Isotopic Age of Enderbites in the Bug Area," Dokl. Akad. Nauk SSSR **263**, 159–162 (1982).
6. E. V. Bibikova, I. Williams, and W. Compston, "Opportunities of Local Ion Microprobe Isotopic Analysis of Zircons in Deciphering the Early History of the Earth as Exemplified by the Novopavlovskii Complex of the Ukrainian Shield," in *Isotopic Geochemistry and Cosmochemistry* (Nauka, Moscow, 1990), pp. 85–102 [in Russian].
7. S. Claesson, E. V. Bibikova, S. Bogdanova, and V. Skobelev, Archaean Terranes, Paleoproterozoic Reworking and Accretion in the Ukrainian Shield, East European Craton, in *European Lithosphere Dynamics*, Geol. Soc. London, Mem. **32**, 645–654 (2006).
8. D. J. De Paolo, "Neodymium Isotopes in the Colorado Front Range and Crust–Mantle Evolution in the Proterozoic," Nature **291**, 193–196 (1981).
9. O. L. Einor, K. E. Esipchuk, and V. A. Tsukanov, *Precambrian of the Western Azov Region* (Kiev. Univ., Kiev, 1971) [in Russian].
10. K. E. Esipchuk, "Stratigraphy and Geochemistry of the Early Precambrian: Problems of Interrelations," Mineral. Zh. **26** (3), 88–99 (2004).
11. *Geological Map and Map of the Crystalline Basement Exposures. Scale 1: 200000, Central Ukrainian Group. L-37-VII (Berdyans'k)*, Ed. by B. V. Borodinya and E. B. Glevassky (State Geol. Survey. Ukr. Ministry of Ecology and Natural Resources Ukraine, Kiev, 1998).
12. E. B. Glevassky and A. M. Glevasska, "The Ukrainian Shield: Precambrian Regional Structure and Paleogeodynamics," Mineral. J. (Ukraine) **24** (4), 47–57 (2002).
13. M. T. Gomez-Pugnaire, P. Ulmer, and V. Lopez-Sanches Vizcaino, "Petrogenesis of the Mafic Igneous Rocks of the Betic Cordilleras: A Field, Petrological and Geochemical Study," Contrib. Mineral. Petrol. **139**, 436–457 (2000).
14. A. W. Hofmann, *Sampling Mantle Heterogeneity through Oceanic Basalts: Isotopes and Trace Elements*, Treaties on Geochemistry, Ed. by H. D. Holland and K. K. Turekian (Elsevier, Amsterdam, 2003).
15. O. S. Ivanushko, "Structural Position and Genesis of Dikes of the Lamprophyre Formation of the Obitochnaya River Basin," Dokl. Akad. Nauk Ukr. SSR, Ser. B., No. 10, 879–883 (1973).
16. S. B. Jacobsen and G. J. Wasserburg, "Sm–Nd Evolution of Chondrites and Achondrites," Earth Planet. Sci. Lett. **67**, 137–150 (1984).
17. V. P. Kirilyuk, A. M. Lysak, and V. Ya. Velikanov, "Basic Features of the Early Precambrian Tectonics of the Ukrainian Shield," Mineral. J. (Ukraine) **24** (4), 39–46 (2002).
18. I. Kushiro, "Effect of Water on the Composition of Magmas Formed at High Pressures," J. Petrol. **13**, 311–334 (1972).
19. S. B. Lobach-Zhuchenko, H. R. Rollinson, V. P. Chekulaev, et al., "The Archaean Sanukitoid Series of the Baltic Shield: Geological Setting, Geochemical Characteristics and Implication for their Genesis," Lithos. **79**, 107–128 (2005).
20. K. R. Ludwig, "ISOPLOT/EX (version 2.00): A Geochronological Toolkit for Microsoft Excel," Geochronol. Center Berkley Spec. Publ., No. 1a, (1999).
21. H. Martin, "The Archaean Grey Gneisses and the Genesis of the Continental Crust," in *Archaean Crustal Evolution*, Ed. by K. C. Condie (Elsevier, Amsterdam, 1994).
22. A. G. Nasad, P. I. Pigulevskii, V. M. Kichurchak, and B. Z. Berzenin, "On the Problem of Complexation Geophysical Materials during Compiling Medium-Scale Maps of Precambrian Complexes with Reference to Middle Dnieper and Priazovskii Geoblocks of the Ukrainian Shield," in *Proceedings of Regional Geological Studies in Ukraine and Genetic Problems. State Geological Map 200* (Kiev, 2001), pp. 64–66 [in Russian].
23. *Petrology, Geochemistry, and Ore Potential of the Intrusive Granitoids of the Ukrainian Shield*, Ed. by I. B. Shcherbakov (Naukova Dumka, Kiev, 1990) [in Russian].
24. R. M. Polunovskii and K. E. Esipchuk, "Central Azov Group," in *Precambrian Stratigraphic Sections of the Ukrainian Shield* (Naukova Dumka, Kiev, 1985), pp. 79–89 [in Russian].
25. P. Richard, N. Shimizi, and C. J. Allegre, "$^{143}Nd/^{144}Nd$—a Natural Tracer: An Application to Ocean Basalts," Earth Planet. Sci. Lett. **31**, 269–278 (1976).
26. A. V. Samsonov, I. V. Chernyshev A. P. Nutman, and W. Compston, "Evolution of the Archaean Aulian Gneiss Complex, Middle Dnieper Gneiss-Greenstone Terrain, Ukrainian Shield: SHRIMP U–Pb Zircon Evidence," Precambrian Res. **78**, 65–78 (1996).
27. C. Sen C. and T. Dunn, "Experimental Model Metasomatism in a Spinel Lherzolite and Production of Amphibole-Bearing Peridotite," Contrib. Mineral. Petrol. **119**, 422–432 (1994).
28. N. P. Shcherbak, E. N. Bartnitskii, and I. P. Lugovaya, *Isotopic Geology of Ukraine* (Naukova Dumka, Kiev, 1981) [in Russian].
29. N. P. Shcherbak, G. V. Artemenko, I. M. Lesnaya, and A. N. Ponomarenko, *Geochronology of the Early Precambrian of the Ukrainian Shield* (Naukova Dumka, Kiev, 2005) [in Russian].
30. N. P. Shcherbak, V. N. Zagnitko, G. V. Artemenko, and E. N. Bartnitskii, "Geochronology of Major Geological Events in the Azov Block of the Ukrainian Shield," Geokhimiya Rudoobrazovanie, No. 21, 112–129 (1995).
31. R. Stern and G. Hanson, "Archean High-Mg Granodiorite: A Derivation of Light Rare Earth Element-Enriched Monzodiorite of Mantle Origin," J. Petrol. **32**, 201–238 (1991).

32. V. A. Tsukanov, *Petrology of Early Precambrian Granitoids in the Azov Region* (Naukova Dumka, Kiev, 1977) [in Russian].

33. I. S. Usenko, *Basic and Ultrabasic Rocks of the Western Azov Region* (Izd-vo AN USSR, Kiev, 1960) [in Russian].

34. M. Whitehouse, S. Claesson, T. Sunde, and J. Vestin, "Ion Microprobe U–Pb Zircon Geochronology and Correlation of Archaean Gneisses from the Lewisian Complex of Gruinard Bay, Northwest Scotland," Geochim. Cosmochim. Acta. **61**, 4429–4438 (1997).

35. M. J. Whitehouse, B. S. Kamber, and S. Moorbath, "Age Significance of U–Th–Pb Zircon Data from Early Archaean Rocks of West Greenland—A Reassessment Based on Combined Ion-Microprobe and Imaging Studies," Chem. Geol. **160**, 201–224 (1999).